

Phase Transitions in Diffusion of Light

Roxana Rezvani Naraghi^{1,2} and Aristide Dogariu^{1,*}

¹CREOL, The College of Optics and Photonics, University of Central Florida, Orlando, Florida 32816, USA

²Department of Physics, University of Central Florida, 4000 Central Florida Boulevard, Orlando, Florida 32816, USA

(Received 17 October 2016; published 21 December 2016)

It has been a long time belief that, with increasing the scattering strength of multiple scattering media, the transport of light gradually slows down and, eventually, comes to a halt corresponding to a localized state. Here we present experimental evidence that different stages emerge in this evolution, which cannot be described by classical diffusion with conventional scaling arguments. A microscopic model captures the relevant aspects of electromagnetic wave propagation and explains the competing mechanisms that prevent the three-dimensional wave localization. We demonstrate that strong evanescent-field couplings hinder the localization of wave resonances and, therefore, impede the slowing down of diffusion. The emerging out of equilibrium steady-state process resembles the diffusion of classical particles in spatially correlated random potentials and the thermalization of matter waves due to atomic collisions.

DOI: 10.1103/PhysRevLett.117.263901

Regimes of electromagnetic (EM) wave propagation range from quasiballistics to diffusive to different kinds of anomalous diffusion including the progression towards a complete arrest of propagation [1,2,3]. Nevertheless, describing the complicated multiple scattering processes requires significant simplifications. A careful examination of aspects specific to EM fields has recently led to the discovery of new phenomena [4,5,6].

When EM waves encounter complex media, the properties of emerging radiation depend not only on the *structural characteristics* of the material system but also on the *scales of interaction* (temporal and spatial). Evidence for different regimes of propagation is routinely presented by modifying material systems and examining the corresponding forms of interaction [7,8]. The effect of the interaction scales is analyzed by imposing macroscopic constraints on the size of the system, which usually leads to complications unrelated to the intrinsic nature of interaction, e.g., boundary effects [9,10,11].

In fact, the properties of EM fields evolve as the radiation penetrates deeper into a medium. The simplest example is the gradual change from ballistic to diffusive regimes of propagation [12,13,14]. Here we will show that light encounters different stages of evolution even in its diffusive propagation. We will demonstrate that these “*phase transitions*” in the transport of light are direct consequences of competing mechanisms of interaction between light and complex media.

When disregarding the wave properties of light, the diffusive transport can be modeled as a random walk of photons with an associated diffusion coefficient D describing the root mean square spread of the photon density [3,15]. In a lossless, semi-infinite medium, the path-length distribution of photons returning to the same location of an impulsive source is $p(s) \propto D^{-(3/2)}s^{-(5/2)} \exp(-z_e^2/4Ds)$,

where z_e accounts for boundary-specific effects [16]. For asymptotically large s , the $-5/2$ power-law decay represents the hallmark of “*normal*” photon diffusion. Examples are plentiful ranging from random lasing [17] to image reconstruction, biology, and medicine [18,19].

First transition: From normal to anomalous diffusion.— In strongly multiply scattering media, wave properties cannot be neglected anymore. Constituent scatterers start acting collectively, modifying the nature of local interferences. Moreover, waves can propagate along reciprocal multiple scattering paths, generating additional interferences seen as closed loops in their trajectories [20,21,22]. This increased probability of returning to the starting point effectively slows down the normal diffusion.

Aside from the deterministic account of diffusion, light propagation can be described stochastically as a random walk of photons. Then, a departure from normal diffusion is portrayed as an anomalous distribution of scattering steps leading to superdiffusion [23] or as a distribution of waiting times before random jumps occur. The latter is due to either long dwell times (scattering resonances) or looping (recurrent scattering), rendering the propagation subdiffusive [24,25].

The slowing down of normal diffusion encountered in strongly scattering media can be modeled as a scale-dependent diffusion process. Based on the scaling theory of localization, the optical diffusion coefficient varies with the size L of the system as $D = D_0 l (1/\xi + 1/L + 1/L_a)$, where l is the transport mean free path while ξ and L_a are the coherence and absorption lengths, respectively [26,27,28]. In reflection, the effective size L of the explored medium is determined by the root mean square (rms) distribution of the energy spread $R = \sqrt{6Dt}$. Thus before reaching localization, $L \ll \xi$, for lossless systems one could show that the path-dependent diffusion coefficient

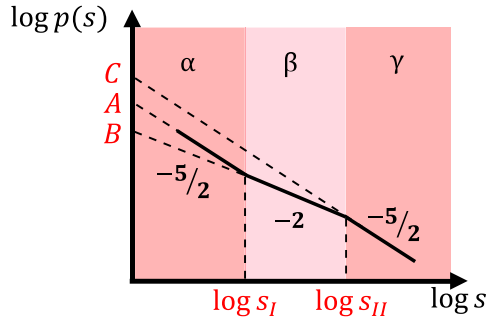


FIG. 1. Distinct regimes of light propagation are characterized by path-length distributions having specific power-law dependences. Phase transitions may occur between normal (α , γ) and anomalous (β) diffusions.

becomes $D(s) \propto (D_0^2 l^2)^{1/3} s^{-1/3}$, which for, large s , leads to $\log[p(s)] = B - 2 \log(s)$. In this regime the diffusion is anomalous, and the path-length distribution decays as s^{-2} . As depicted in Fig. 1, this change in the $p(s)$ behavior indicates the first phase transition in the diffusion of light: from normal to anomalous.

Second transition: From anomalous back to normal.—In densely packed composite media, the individual scatterers are in close proximity and become optically connected through strong near-field (NF) interactions. This situation leads to a new regime of transport where the energy diffuses also through additional evanescent channels [5]. Moreover, reports also suggest that the vector character of light has a critical role in establishing this interaction regime [4,6]. All these very recent developments may help clarify the elusive strong localization of light in three-dimensional photonic structures [29].

At high concentrations, the recurrent scattering sequences discussed before can be imagined as loops of energy flows inside the medium, which determine the overall subdiffusive nature of energy transport. The NF coupling, on the other hand, has the tendency to destroy these loops by leaking energy into new channels [5]. The longer the paths inside the medium, the more loops can be created. However, the NF events are also more probable, and, as a result, the loops of energy flows are destroyed more and more, and the diffusive propagation gradually returns to normal. This constitutes a second phase transition in the diffusion of light: from anomalous to normal.

The evolution of path-length distribution through these phase transitions is generically depicted in Fig. 1. Let us now comment on the meaning of the extrapolation constants A and C . It is easy to show that $A, (C) = \log[(4\pi D_{A,(C)})^{-3/2} z_e]$, where D_A and D_C are the normal diffusion coefficients before the first and after the second transition, respectively. It is evident that $D_C < D_A$. This means that, even though the normal diffusion is eventually recovered, because of the slowing down at intermediate ranges, light practically expands over larger areas at a lower pace than if the diffusion

would have been normal all along. This could open up new possibilities to control the large scale propagation.

We also note that for any diffusion, including the “passive” diffusion of photons, one can associate an effective temperature at which the process evolves [30]. Then, the return to normality in the region (γ) corresponds to reaching the thermodynamic equilibrium at large scales. Moreover, one can argue that the diffusing photons reach thermodynamic equilibrium at lower effective temperatures because of the “cooling down” during the evolution at intermediate scales (β).

The other extrapolation constant in Fig. 1 is $B = \log\{[4\pi(D_A^2 l^2/6)^{1/3}]^{-3/2} z_e\}$, and, from $A - B \propto \log(s_I)$, it follows that $\log s_I \propto l^2/D_A$. It is interesting to note that $C - B \propto \log s_{II}$ measures in fact the “duration” or the spatial extent of the anomalous diffusion $s_{II} = s_I (D_A/D_C)^3$, which is accessible experimentally as we will show in the following.

Experimental demonstration.—The subdiffusive behavior of light has been demonstrated in a number of photonic structures [28]. Here we establish experimentally the presence of the second phase transition. Usually, light transport in disordered scattering media is examined by techniques providing macroscopically averaged properties such as transmission. Thus, one cannot say much about the way the diffusion evolves in the steady state. Clarifying this evolution requires access to detailed information about the distribution of paths the optical waves take throughout the medium. A direct measurements of the probability density function of radiation path lengths can be performed interferometrically [31].

Using a broadband light source in conjunction with a single-mode fiber-optic-based Michelson interferometer as illustrated in Fig. 2, we directly infer the distribution of path lengths of multiply scattered light. Notably, dynamic ranges of more than 5 orders of magnitude can be readily obtained with a corresponding temporal resolution of 30 fs. In back-scattering from semi-infinite media, the coherence gating

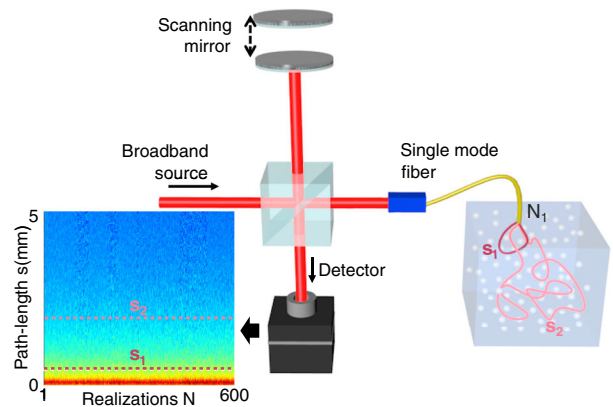


FIG. 2. A single-mode fiber-based low-coherence interferometer allows the direct measurement of pathlength distributions in reflection from a semi-infinite medium. An ensemble average is created over measurements at different locations.

permits isolating the contribution from optical paths of specified length s , and, therefore, the corresponding probability density $p(s)$ is directly determined. The measurement configuration corresponds to the situation where the point source and point detector coincide. An ensemble average is constructed over realizations of the medium or over measurements at different locations as suggested in Fig. 2.

To study systematically the occurrence of these phase transitions, we examined solid media which were specifically designed to maintain prescribed volume fractions of well-dispersed, alumina surface-treated TiO₂ submicron particles. Here we present data on samples composed of 5%–50% volume fractions of 300 nm diameter TiO₂ particles (DuPont, R-706), embedded into a polymer matrix with a refractive index of 1.5. Spectra were recorded using a broadband source with a bandwidth of 30 nm centered on a wavelength of 1310 nm. Measurements were performed over more than 600 different regions of the samples, to ensure the appropriate ensemble average.

The main results are summarized in Fig. 3. As explained before, the optical path-length distribution associated with normal diffusion through a semi-infinite medium should exhibit an $s^{-5/2}$ asymptotic dependence. This is exactly what is observed for low TiO₂ concentrations for more than two decades of path lengths. However, as the concentration of particles increases, this behavior begins to change: In the short path-length domain, the power-law exponent starts to deviate from $-5/2$ and approaches -2 . This evolution towards a time-dependent diffusion coefficient is anticipated according to theories on wave localization, as we discussed before [28]. The progression is more evident as the TiO₂ concentration increases, indicating significant contributions from recurrent scattering or loops of energy flows. This unmistakable subdiffusive behavior of light propagation in 3D random media is a clear signature of an incipient regime where coherent wave effects cannot be neglected anymore.

The most remarkable in Fig. 3 is nevertheless the conversion back to an asymptotic $s^{-5/2}$ decay. This crossover represents the first experimental evidence for the second phase transition from anomalous back to normal diffusion, which we anticipated in the preceding discussion. Recovering the diffusive behavior for longer optical paths is a consequence of the trade-off between the competing mechanisms of recurrent scattering and NF coupling, as we will discuss in the following.

Discussion.—Let us now discuss in more detail the conditions in which these two phase transitions occur. The probability for a wave to return close to its starting point (recurrent scattering) should be independent of the geometry of a measurement. This probability is determined solely by the ratio between the trajectory volume and the volume the light explores inside the multiple scattering medium [32]. In reflection from a semi-infinite medium, longer paths penetrate through larger volumes, and, therefore, the size

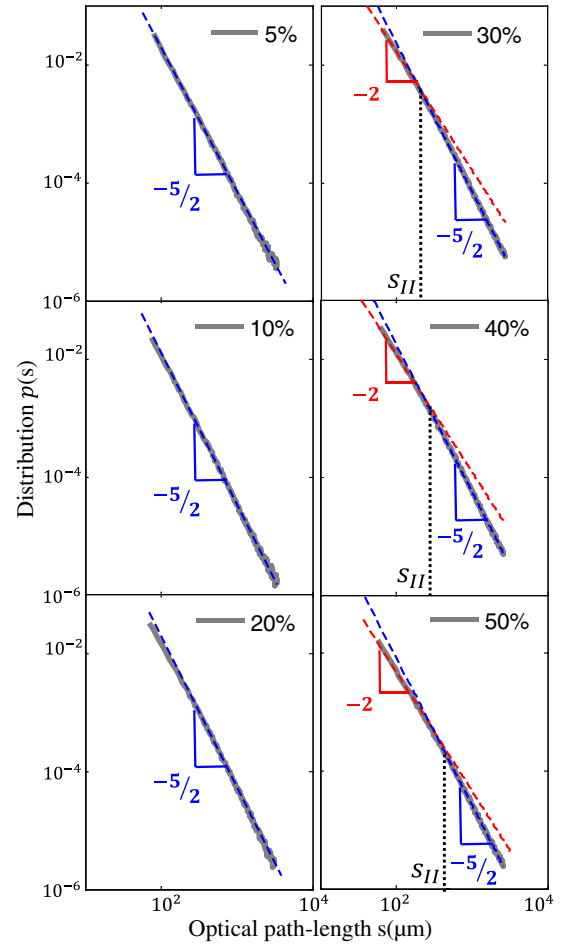


FIG. 3. Experimental probability distributions of path lengths corresponding to semi-infinite random media comprising dispersions of TiO₂ particles with different volume fractions as indicated. The blue and red dashed lines indicate the normal and the subdiffusive regimes, respectively. The dotted lines at 233.6, 326.7, and 395.9 μm indicate the s_{II} values corresponding to 30%, 40%, and 50% volume fractions of TiO₂ particles, respectively.

of the explored medium evolves as $V_m(s) \propto L^3(s)$. The linear scale of this medium expands as $L(t) = \sqrt{6D(t)t}$ with a diffusion coefficient $D(t) = (D_B^2 l^2 / 6)^{1/3} t^{-1/3}$. It then follows that $L(t) = [6(D_B^2 l^2 / 6)^{1/3} t^{-1/3} t]^{1/2} = \sqrt[3]{6} D_B l t^{1/3}$, which, in terms of the length of trajectories, means that $L^3(s) = 6(D_B l)s/c$. In these conditions, the probability of recurrent scattering becomes

$$p_{\times} = \frac{V_{tr}}{V_{m(s)}} = \frac{\lambda^2 s}{L^3} = \frac{c \lambda^2}{6 l D_B} = \frac{\lambda^2}{2 l^2}, \quad (1)$$

which, notably, is independent of the path length, because, in reflection, there are no constraints on possible trajectories. The situation is quite different when the size of the explored medium is a constant V , as in the case of transmission measurements. The probability of a trajectory crossing in this

case is given by $p_{\times} = V_{tr}/V = \lambda^2 s/V \propto s$, which depends linearly on the length of trajectories because of the macroscopic constraint imposed by the finite size of the medium.

Let us now analyze the near-field coupling, the competing mechanism that inhibits recurrent scattering. At high volume fractions of particles, the energy can leak out of the diffusive channels because of the near-field interactions between scatterers situated at less than a wavelength apart. To determine the associated probability, let us consider a typical propagation channel of length s and cross section λ^2 . Because of NF interactions, energy can leak out of this channel at s/λ locations. The strength of NF coupling to particles outside the trajectory is measured by the total area A_{NF} of potential interactions, which, in turn, is determined by the size of the near-field cross section σ_{NF} and the number of such possible events. In other words, $A_{NF} = \sigma_{NF}(3n_0\lambda^3)$. Note that, aside from optical size, the near-field cross section $\bar{\sigma}_{NF}$ accounts for angular and polarization averaging [5].

At each location along the trajectory, the NF coupling process happens with an efficiency dictated by the ratio between A_{NF} and the total area $A = 2\pi\lambda^2$ surrounding a typical location. Thus, the probability of energy leaking along the entire trajectory of length s is

$$P_{\text{leak}} = \frac{3\pi n_0 \lambda^3 \times \sigma_{NF} s}{2\pi \lambda^2} \frac{s}{\lambda} = \frac{3}{2} n_0 \bar{\sigma}_{NF} s, \quad (2)$$

which does increase with the length of the trajectory as opposed to the crossing probability in Eq. (1). This means that, as the path length through the medium grows, the rate at which loops are destroyed can exceed the rate at which they are created. Eventually, the ‘‘anomaly’’ caused by recurrent scattering ceases and the diffusion recovers its normal behavior with a diffusion constant that is scale independent. This is the second phase transition of light. The different stages of transport evolution are schematically illustrated in Fig. 4.

It is also instructive to examine these two probabilities in the context of the number density of scattering centers. Clearly, because $l \sim 1/n_0$, the probability of recurrent scattering p_{\times} in Eq. (1) depends quadratically on concentration, $p_{\times} \sim n_0^2$. The leaking probability, on the other hand, grows linearly with both n_0 and s , $p_{\text{leak}} \sim sn_0$ as seen in Eq. (2). As the threshold for the second phase transition can be set when these two probabilities become comparable, it follows that

$$s_{II} = \frac{2\lambda^2 \sigma^2 n_0}{3\bar{\sigma}_{NF}}. \quad (3)$$

It can be concluded that this transition happens at larger and larger path lengths when n_0 increases, as we also observed experimentally. When using Eq. (3) for 30%, 40%, and 50% volume fractions of spherical TiO_2 particles, one finds that s_{II} is, respectively, 227.7, 303.6,

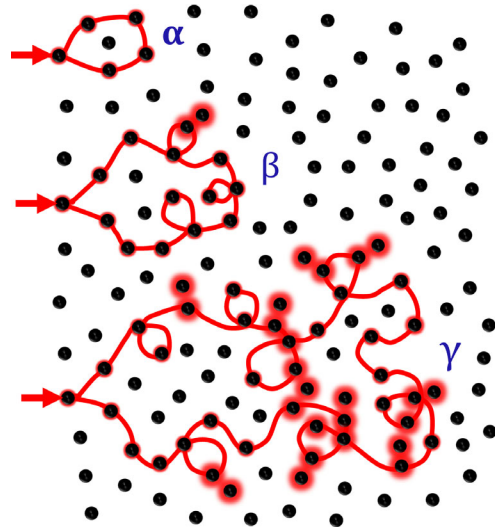


FIG. 4. Competing mechanisms of interaction dominate different stages of transport evolution. Initially, at scales (α) the wave expands normally but then, at larger scales (β), loops of energy flow are created with a certain probability. The competing mechanism of energy leaking destroys these loops and dominates at even larger scales (γ) of interaction.

and $379.5 \mu\text{m}$, in very good agreement with the s_{II} extracted experimentally and shown in Fig. 3.

In closing, we comment on diffusion as a general concept associated with evolution. Most common is, of course, the particle diffusion starting from the Brownian one, but the concept expands from social phenomena to, of course, waves. Waves bring in certain specific manifestations, but the parallel with particle diffusion is always meaningful and instructive. In this context, the two phase transitions in the diffusion of light discussed here bear a strong similarity to the phenomenon of particle diffusion in spatially correlated random potentials [33–36]. At short times, particles execute a free, Brownian-like diffusion before encountering any influence from the external, constraining potential. However, once the spatial dispersion reaches scales comparable with the correlation length of this potential, the diffusion starts to slow down. One could argue that, at these intermediate scales, the particles’ diffusion is somewhat ‘‘caged.’’ This can happen because an externally applied random potential [37–39], structural inhomogeneity of gel-like media through which particles diffuse [40–42], or simply because of the direct influence of particle crowding [43,44]. In the long-time limit, the particles eventually tunnel through these potential cages and the normal diffusion recovers, as expected at the asymptotic thermodynamic equilibrium. These three regimes of diffusion are equivalent to the three stages of path-length evolution depicted in Figs. 1 and 4.

The different evolution stages of EM wave transport also bear similarities to the thermalization of matter waves due to atomic collisions. In this case, even for a weak

interaction, an atomic cloud released in a disordered potential never reaches a localized stationary state [45].

Conclusions.—Our results demonstrate the existence of unexplored regimes for wave propagation through complex media. Going beyond traditional random walk descriptions, the circumstances we created provide access to new aspects of the universal process of diffusion in external potentials.

The process is similar to the diffusion of particles subjected to additional time-dependent random potentials. In the case of electromagnetic waves, the locally strong interferences create an effective random potential that constrains the overall diffusion of waves. Our results demonstrate that the average residence time in this confining potential is regulated by the strength of the inherent evanescent coupling between microscopic elements of the complex medium. In particular, we have shown that strong recurrent scattering due to on-shell propagating fields is impeded by strongly localized evanescent couplings (off-shell wave manifestations). The fact that the transport of optical waves cannot slow down indefinitely is of high relevance for the elusive Anderson localization of light in three-dimensional media [46].

We presented a microscopic model that describes the diffusion of electromagnetic waves in random media and provides a familiar thermodynamical description similar to an equilibrium fluctuation-dissipation relation. Aside from its fundamental relevance, understanding all the wave aspects governing such interactions could lead to new means to engineer materials where the nature and the extent of anomalous transport can be controlled at will.

-
- [1] P. Sheng, *Scattering and Localization of Classical Waves in Random Media* (World Scientific, Singapore, 1990).
- [2] S. John, *Phys. Rev. B* **31**, 304 (1985).
- [3] A. Ishimaru, *Wave Propagation and Scattering in Random Media* (Academic Press, New York 1978).
- [4] S. E. Skipetrov and I. M. Sokolov, *Phys. Rev. Lett.* **112**, 023905 (2014).
- [5] R. R. Naraghi, S. Sukhov, J. J. Sáenz, and A. Dogariu, *Phys. Rev. Lett.* **115**, 203903 (2015).
- [6] N. Cherroret, D. Delande, and B. A. van Tiggelen, *Phys. Rev. A* **94**, 012702 (2016).
- [7] M. D. Birowosuto, S. E. Skipetrov, W. L. Vos, and A. P. Mosk, *Phys. Rev. Lett.* **105**, 013904 (2010).
- [8] V. Krachmalnicoff, E. Castanié, Y. De Wilde, and R. Carminati, *Phys. Rev. Lett.* **105**, 183901 (2010).
- [9] E. Amic, J. M. Luck, and T. M. Nieuwenhuizen, *J. Phys. A* **29**, 4915 (1996).
- [10] G. Popescu, C. Mujat, and A. Dogariu, *Phys. Rev. E* **61**, 4523 (2000).
- [11] M. Xu, W. Cai, M. Lax, and R. R. Alfano, *Phys. Rev. E* **65**, 066609 (2002).
- [12] K. M. Yoo, F. Liu, and R. R. Alfano, *Phys. Rev. Lett.* **64**, 2647 (1990).
- [13] R. Elaloufi, R. Carminati, and J. J. Greffet, *J. Opt. Soc. Am. A* **21**, 1430 (2004).
- [14] A. Yaroshevsky, Z. Glasser, E. E. Granot, and S. Sternklar, *Opt. Lett.* **36**, 1395 (2011).
- [15] M. V. van Rossum and T. M. Nieuwenhuizen, *Rev. Mod. Phys.* **71**, 313 (1999).
- [16] M. S. Patterson, B. Chance, and B. C. Wilson, *Appl. Opt.* **28**, 2331 (1989).
- [17] H. Cao, Y. G. Zhao, S. T. Ho, E. W. Seelig, Q. H. Wang, and R. P. Chang, *Phys. Rev. Lett.* **82**, 2278 (1999).
- [18] V. Ntziachristos, J. Ripoll, L. V. Wang, and R. Weissleder, *Nat. Biotechnol.* **23**, 313 (2005).
- [19] T. Durduran, R. Choe, W. B. Baker, and A. G. Yodh, *Rep. Prog. Phys.* **73**, 076701 (2010).
- [20] M. Störzer, P. Gross, C. M. Aegerter, and G. Maret, *Phys. Rev. Lett.* **96**, 063904 (2006).
- [21] D. S. Wiersma, M. P. van Albada, B. A. van Tiggelen, and A. Lagendijk, *Phys. Rev. Lett.* **74**, 4193 (1995).
- [22] A. Aubry, L. A. Cobus, S. E. Skipetrov, B. A. Van Tiggelen, A. Derode, and J. H. Page, *Phys. Rev. Lett.* **112**, 043903 (2014).
- [23] P. Barthelemy, J. Bertolotti, and D. S. Wiersma, *Nature (London)* **453**, 495 (2008).
- [24] G. Cwilich and Y. Fu, *Phys. Rev. B* **46**, 12015 (1992).
- [25] M. P. van Albada, B. A. van Tiggelen, A. Lagendijk, and A. Tip, *Phys. Rev. Lett.* **66**, 3132 (1991).
- [26] P. W. Anderson, *Philos. Mag. B* **52**, 505 (1985).
- [27] S. John, *Phys. Rev. Lett.* **53**, 2169 (1984).
- [28] K. M. Douglass, S. John, T. Suezaki, G. A. Ozin, and A. Dogariu, *Opt. Express* **19**, 25320 (2011).
- [29] T. Sperling, L. Schertel, M. Ackermann, G. J. Aubry, C. M. Aegerter, and G. Maret, *New J. Phys.* **18**, 013039 (2016).
- [30] L. F. Cugliandolo, *J. Phys. A* **44**, 483001 (2011).
- [31] G. Popescu and A. Dogariu, *Opt. Lett.* **24**, 442 (1999).
- [32] E. Akkermans and G. Montambaux, *J. Opt. Soc. Am. B* **21**, 101 (2004).
- [33] R. Zwanzig, *Proc. Natl. Acad. Sci. U.S.A.* **85**, 2029 (1988).
- [34] M. A. Desposito, *Phys. Rev. E* **84**, 061114 (2011).
- [35] P. Tierno, F. Sagués, T. H. Johansen, and I. M. Sokolov, *Phys. Rev. Lett.* **109**, 070601 (2012).
- [36] R. D. Hanes, M. Schmiedeberg, and S. U. Egelhaaf, *Phys. Rev. E* **88**, 062133 (2013).
- [37] A. H. Romero and J. M. Sancho, *Phys. Rev. E* **58**, 2833 (1998).
- [38] F. Jendrzejewski, A. Bernard, K. Mueller, P. Cheinet, V. Josse, M. Piraud, L. Pezzé, L. Sanchez-Palencia, A. Aspect, and P. Bouyer, *Nat. Phys.* **8**, 398 (2012).
- [39] K. M. Douglass, S. Sukhov, and A. Dogariu, *Nat. Photonics* **6**, 834 (2012).
- [40] R. M. Dickson, D. J. Norris, Y. L. Tzeng, and W. E. Moerner, *Science* **274**, 966 (1996).
- [41] W. Liang, J. R. Guman-Sepulveda, S. He, A. Dogariu, and J. Y. Fang, *J. Mater. Sci. Chem. Eng.* **3**, 6 (2015).
- [42] J. Guzman-Sepulveda, J. Deng, J. Fang, and A. Dogariu (to be published).
- [43] M. Weiss, M. Elsner, F. Kartberg, and T. Nilsson, *Biophys. J.* **87**, 3518 (2004).
- [44] F. Höfling and T. Franosch, *Rep. Prog. Phys.* **76**, 046602 (2013).
- [45] N. Cherroret, T. Karpiuk, B. Grémaud, and C. Miniatura, *Phys. Rev. A* **92**, 063614 (2015).
- [46] S. E. Skipetrov and J. H. Page, *New J. Phys.* **18**, 021001 (2016).